Structural diversity of frameshifting signals : reprogramming the programmed

Yu, C.H.

Chapter VI

Comparison of $preQ_1$ riboswitches by molecular dynamics simulations and ribosomal frameshifting: identification of a novel RNA-ligand interaction

Chien-Hung Yu[1]*, Jinghui Luo[2]*, Shina C. L. Kamerlin[3], Jan Pieter Abrahams[2], René C.L. Olsthoorn[1]

*contributed equally

[1]Department of Molecular Genetics and [2]Biophysical Structural Chemistry, Leiden Institute of Chemistry, Leiden University, PO Box 9502, Leiden, The Netherlands.
[3]Department of Cell and Molecular Biology (ICM), Uppsala University, BMC, Box 596, S-751 24 Uppsala, Sweden.

Manuscript in preparation

Abstract

$PreQ_1$ riboswitches are the smallest riboswitch found to date that function as genetic control elements upon binding the metabolite molecule 7-aminomethyl-7-deazaguanine ($preQ_1$), an intermediate in queuosine (Q) biosynthesis. With only 34 nucleotides (nts), $preQ_1$ riboswitch aptamers display high affinities for their cognate ligand, binding of which stabilizes the formation of a compact RNA pseudoknot. Here we have developed a novel ligand-dependent *in vitro* assay, based on ribosomal frameshifting, to investigate the molecular basis of the $preQ_1$ affinity of two distinct $preQ_1$ aptamers uncoupled from their expression platforms. Our data show that *Bacillus subtilis* (*B. subtilis*) and *Fusobacterium nucleatum* (*F. nucleatum*) $preQ_1$ aptamers differ in their ability to act as frameshifter pseudoknots due to differences in

preQ$_1$ affinity. Molecular dynamics (MD) simulations, using the published coordinates of the *B. subtilis* aptamer, revealed the possibility of additional contacts between preQ$_1$ and residue G7 in the *F. nucleatum* aptamer. These contacts are absent in the *B. subtilis* aptamer where the corresponding residue is a U. Swapping the identity of the 7th nucleotide between both preQ$_1$ aptamers decreased the ligand-dependent frameshifting of the *F. nucleatum* pseudoknot more than 5-fold but increased the sensitivity of the *B. subtilis* one more than 5-fold. These data show that MD simulation is a valuable tool to investigate molecular details of RNA-ligand interactions. Combined with the high sensitivity of the *in vitro* ribosomal frameshifting assay, this study forms the basis for developing high-throughput assays of riboswitch-metabolite interactions.

Introduction

Riboswitches are non-coding structured RNAs typically located in the 5'-untranslated regions (UTRs) that bind metabolites, such as nucleobases, coenzymes, and amino acids with high specificity and affinity to regulate gene expression (1). Although majorly found in eubacteria, some representatives exist in archaea (2) and eukaryotes (3). Riboswitches typically consist of a metabolite-binding aptamer to sense cellular metabolites to regulate an adjoining expression platform through transcriptional or translational control without assistance of proteins (4). Transcriptional control can be mediated upon metabolite binding either through the formation of a transcription terminator hairpin that stops further elongation by RNA polymerase or through disruption of an existing terminator so that transcription can be resumed. Translational control is thought to occur by metabolite induced structural changes that may expose or sequester the Shine-Dalgarno sequence thereby enabling or inhibiting translation initiation (5).

Metabolite-binding aptamers are formed from highly conserved sequences and/or structural elements. Through genome-wide bioinformatics analysis, several novel riboswitch candidates have been identified, including one that responds to preQ$_1$, a precursor of Q (6). Q is a post-transcriptional modification of the wobble base of GUN anticodons of bacterial and eukaryotic tRNAs and is important in translational fidelity (7). The aptamer domain of the preQ$_1$ riboswitch upstream of the Q biosynthesis operon consists of a minimal sequence of 34 nts and is the smallest riboswitch aptamer known to date. The preQ$_1$ aptamer generally consists of a 5 base pair (bp) stem and a loop of 10-13 nts, followed by a single-stranded region of about 11-14 nts (8) (Fig. 1). In the presence of nanomolar concentrations of preQ$_1$, the

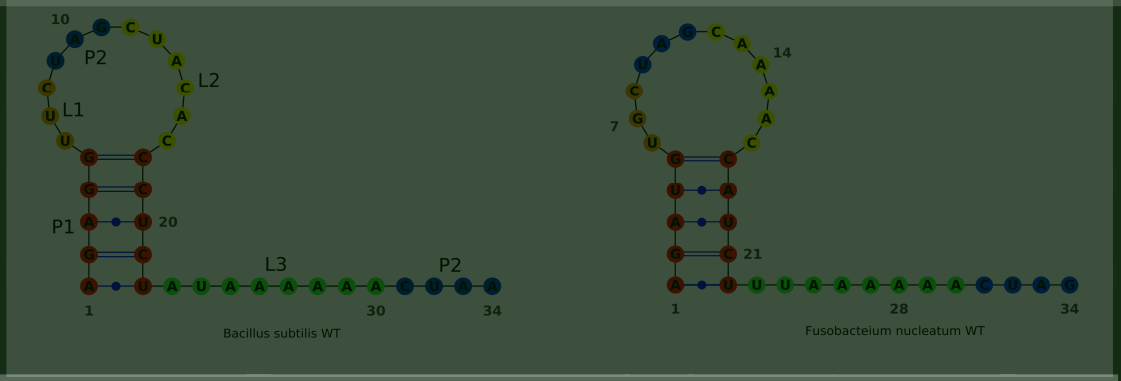

Figure 1. The sequences and secondary structures of preQ$_1$ riboswitch aptamers from *Bacillus subtilis* (left) and *Fusobaterium nucleatem* (right). The colors of red, orange, blue, yellow and green represent stem 1 (P1), loop 1 (L1), stem 2 (P2), loop 2 (L2) and loop 3 (L3), respectively.

aptamers from *B. subtilis* (9,10) *F. nucleatum* (11) and *Thermoanaerobacter tengcongensis* (12) have been shown to fold into a compact pseudoknot by pairing of 3-4 nucleotides from the loop to 3-4 nts from the downstream region.

Programmed ribosomal frameshifting (PRF) is a translational recoding process in which ribosomes can shift 1 nt forward (+1 PRF) or 1 or 2 nts backward (-1 PRF or -2 PRF) on a mRNA and resume translation in a different reading frame [see (13) for a review]. There are two critical *cis*-acting RNA elements responsible for PRF: a slippery sequence and a downstream structural element. This structural element can be either a hairpin or a pseudoknot, and the stability of which is positively correlated with frameshifting efficiency (14). Since the pseudoknot structure, which is formed upon binding of preQ$_1$ to its aptamer, is reminiscent of several frameshift inducing pseudoknots (15), it is of interest to investigate whether the ligand-induced pseudoknot can stimulate PRF as well.

In this report, we explored the ability of *F. nucleatum* and *B. subtilis* preQ$_1$ riboswitch aptamers to function as ligand-dependent pseudoknots in –1 PRF. The stability of both riboswitch aptamers was also investigated by MD simulations. Based on MD observations a novel interaction with preQ$_1$ was predicted and subsequently validated by our frameshift assay. Therefore, our combined MD simulation and frameshift assay provide a platform to understand the structural basis of ligand binding to preQ1 riboswitch aptamers and possibly others as well.

Materials and Methods

Frameshift reporter construction and assays

Minus 1 frameshifting was monitored by the SF reporter construct described earlier

(16). Briefly, complementary oligonucleotides (Eurogentec, Liege, Belgium) were annealed followed by ligation into SpeI/NcoI digested SF vector to obtain experimental constructs (sequences are available upon request). All the constructs were verified by DNA sequencing (LGTC, Leiden, The Netherlands).

Frameshift assays were carried out in rabbit reticulocyte lysates (RRL) (Promega, Benelux, The Netherlands) as reported (17). In short, the target plasmids were linearized by BamHI (Fermentas, The Netherlands) followed by successive phenol/chloroform extraction and ethanol precipitation. The linearized templates were transcribed by SP6 RNA polymerase. The resulting transcripts were electrophoresed in agarose gels to determine their quantity and quality. 5 nM of mRNA were then mixed with 4 µl of RRL, 0.15 µl of ^{35}S methionine [>1000Ci (37.0TBq)/mmol, Easy Tag, PerkinElmer], 0.15 µl 1mM amino acid mix without methionine, and various concentration of preq1 (0~200 µM) in a final volume of 10 µl, and incubated at 30ºC for 1 hour. Note that the $preQ_1$ compound, a generous gift of Dr. Iwata-Reuyl, was first dissolved at a concentration of 200 mM in DMSO, and then diluted to 2mM in RNase free water as our working solution of which 1 µl was added to the translation mixture. We kept the final concentration of DMSO in the translation mixture at 0.1% to prevent adverse effects on translation. After translation, samples were boiled with 2X Laemmli buffer for 3 min and loaded onto 13% SDS-PAGE. Gels were then dried and exposed to phosphoimager screen. The intensity of shifted and non-shifted protein products were quantified by Quantity One (Biorad, The Netherlands). After subtracting the background, the frameshifting efficiency of each construct at each concentration of $preQ_1$ was calculated as: the amount of -1 frameshifted product divided by the sum of the amount of in-frame product and -1 frameshifted product after correction for the number of methionines in each fragment, and then multiplied by 100.

Construction of $preQ_1$ riboswitch aptamer of *F. nucleatum* from known coordinates of *B. subtilis*

The NMR solution structure of $preQ_1$ in complex with the 34 nts long aptamer domain of the $preQ_1$ riboswitch (PDB ID: 2L1V) from *B. subtilis* served as the homology structure for building the $preQ_1$ aptamer of *F. nucleatum* by RNABuilder 2.3 package (18). To predict the structure of $preQ_1$ aptamer of *F. nucleatum*, we first aligned the secondary structure between aptamers from different species, established by comparative sequence analysis based on the NMR structure. Subsequently, the threading force was used to build initial models of the $preQ_1$ aptamer of *F. nucleatum*. Energy minimizations were carried out to remove bad contacts in the initial model of the *F. nucleatum* aptamer with 3000 steps using the steepest descent algorithm followed by 3000 steps with a conjugate gradient algorithm of energy minimization. In addition,

the apo-preQ$_1$ aptamer systems were obtained by removing the preQ$_1$ molecule from the preQ$_1$ aptamer of *B. subtilis* and *F. nucleatum*.

Molecular dynamics simulations

The structures of preQ$_1$ aptamers of *B. subtilis* from NMR and *F. nucleatum* from RNA Builder were used as starting structures for MD simulations. The force field of the preQ$_1$ system was calculated with ANTCHAMBER using the AM1-bcc model and the Leap module in AMBER Tools. Both simulation systems were neutralized with $Mg2^+$ and Cl^- in order to reach 2 mM $Mg2^+$ in solution and solved with TIP3P water molecules in a cubic box, allowing for 12 Å of water around the nucleic acid systems. All simulations were performed in GROMACS 4.5.1 package with the AMBER99 force field. The steepest descent algorithm and conjugate gradient algorithm were implemented for energy minimization of the structures as above, and then each system was equilibrated for 30 ps at 300K by diffusing water around the structures. Simulations were carried out at a constant temperature of 300K and at 1 bar pressure using the Berendsen algorithm and a periodic boundary system. The particle mesh Ewald (PME) method was used to treat long-range interactions. The bond distances and bond angles of the solvent water were constrained via the SETTLE algorithm. Other bond distances were handled via the LINCS algorithm. The resulting trajectories were analyzed with the GROMACS analyze package. The figures were made by Pymol.

Results

PreQ$_1$ riboswitch aptamers from *F. nucleatum* and *B. subtilis* induce -1 PRF to different extents

The characterized preQ$_1$ riboswitch aptamers (9–12) show resemblance to a subset of frameshifting pseudoknot structures (15). Therefore we examined if this kind of ligand-responsive pseudoknot structures can induce -1 PRF using our frameshift reporter system (16). Interestingly, the preQ$_1$ riboswitch aptamer (Fn1) of *F. nucleatum* showed a preQ$_1$ concentration-dependent -1 PRF and reached a significant 20% of frameshifting at 200 µM of preQ$_1$ (Fig. 2b and 2d). Note that a cytidine was inserted into L3 in these constructs to prevent the creation of a premature stop codon. Removal of the 3' part of stem 2 (P2) abolished frameshifting (data not shown), indicating that ligand itself is not responsible for frameshifting but the formation of the pseudoknot is.

With the *B. subtilis* aptamer (Bs1), the induced frameshift efficiency was almost??? 3-fold lower than that of the Fn1 of *F. nucleatum* (Fig. 2a, and 2c), likely as a result of

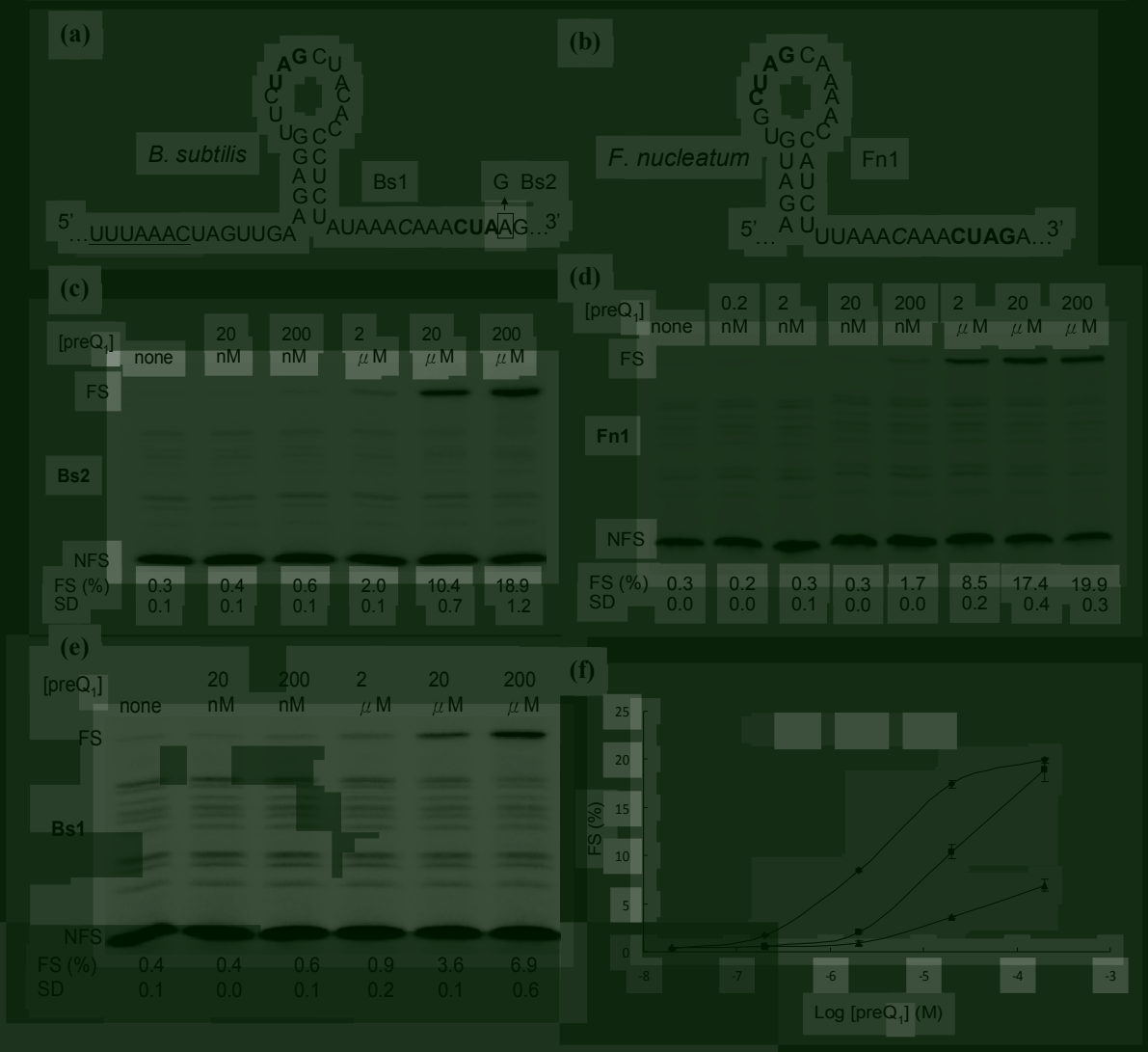

Figure 2. Minus 1 PRF induced by preQ$_1$ riboswitch aptamers. The relevant sequences of the frameshift reporter constructs contained preQ$_1$ aptamers from *B. subtilis* (a) or *F. nucleatum* (b) are shown. The sequences in bold indicate base pairs formed upon ligand binding. The cytidines in italic are the insertions to prevent pre-mature stop codon in frameshift assays. Slippery sequence is underscored. (c-e) SDS-PAGE analysis of ^{35}S-methionine labeled translation products of each frameshift construct in RRL in different preQ$_1$ concentrations of each frameshift construct. The appearance of 65-kD FS product indicates the occurrence of -1 ribosomal frameshifting while the NSF indicates zero-frame product without frameshifting. (f) Graph showing the frameshift efficiency (at the y-axis) induced by each preQ$_1$ riboswitch aptamer construct (Diamond, square, and triangle represent Fn1, Bs2, and Bs1, respectively) at various concentrations of preQ$_1$ compound (at the x-axis). The error bars represent the standard deviation of at least two independent assays. See Materials and Methods for details.

weaker P2 (3 bp vs. v.s 4 bp in *F. nucleatum*). Introduction of a fourth bp in P2 of the *B. subtilis* aptamer (Bs2) to create the same P2 stem as in Fn1, did increase frameshifting to a level similar as of Fn1 at 200μM preQ1 (Fig. 2a and 2e). However,

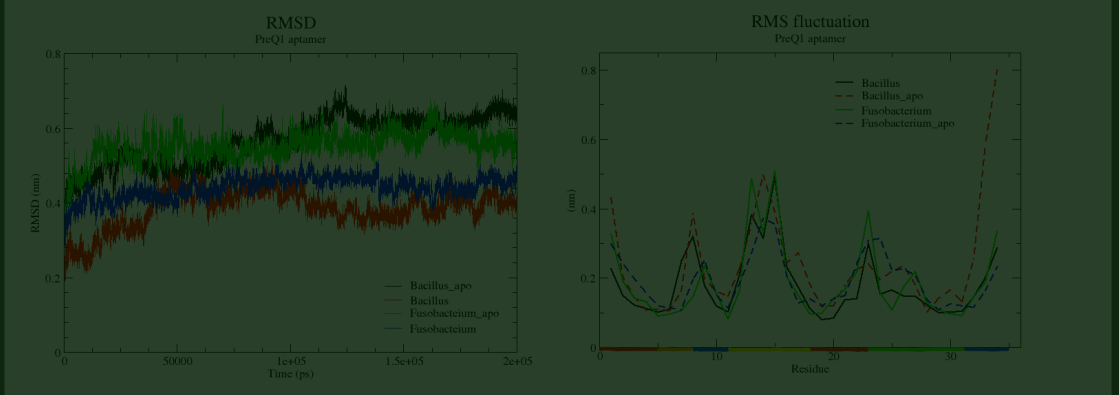

Figure 3. Root mean square deviation (RMSD) (A) (black and red lines indicate apo and bound *B. subtilis* aptamers, respectively; green and blue lines represent apo and bound *F. nucleatum* aptamers, respectively) and root mean square fluctuations (RMSF) (B) (black and green lines indicate bound aptamers of *B. subtilis* and *F.nucleatum,* respectively; red and blue dash lines represent apo aptamers of *B. subtilis* and *F.nucleatum,* respectively) of the preQ$_1$ aptamer system and the Apo-preQ$_1$ aptamer system during 200 ns of molecular dynamics simulation. Loops and stems of aptamers are colored according to the scheme of Figure 1.

the Bs2 aptamer responded more slowly than Fn1 to changes in the preQ1 concentrations (Fig. 2f). The results suggest that, although the overall stability of Fn1 and Bs2 aptamers are similar, they are different in their ligand affinity. To investigate the structural details behind the varied ligand sensitivities of these aptamers, we decided to use computer-assisted MD simulations.

Structure and dynamics comparison of preQ$_1$ aptamers from *B. subtilis* and *F. nucleatum*

Since a high-resolution structure of the *F. nucleatum* preQ$_1$ riboswitch aptamer is not available, we utilized the RNABuilder 2.3 package and the NMR coordinates of the *B. subtilis* preQ1 aptamer solution structure (9, 19) to build a 3D model of the *F. nucleatum* aptamer. Subsequently, a relatively long MD simulation (200 ns) was implemented on the known *B. subtilis* aptamer and the homology structure of the *F. nucleatum* aptamer. Another 200 ns of simulations were carried out on both aptamer structures after removal of preQ$_1$ from the coordinate file. The starting structure and average structure of MD simulations of preQ$_1$-aptamers and apo-preQ$_1$ aptamers from the two species were monitored carefully in order to detect signs of instabilities from coordinates that may result from the modeled structure or simulation parameters.

The root mean square deviations (RMSD) of both aptamers in their ligand-bound or ligand-free state over 200 ns simulation are shown in Figure 3A. The data show that

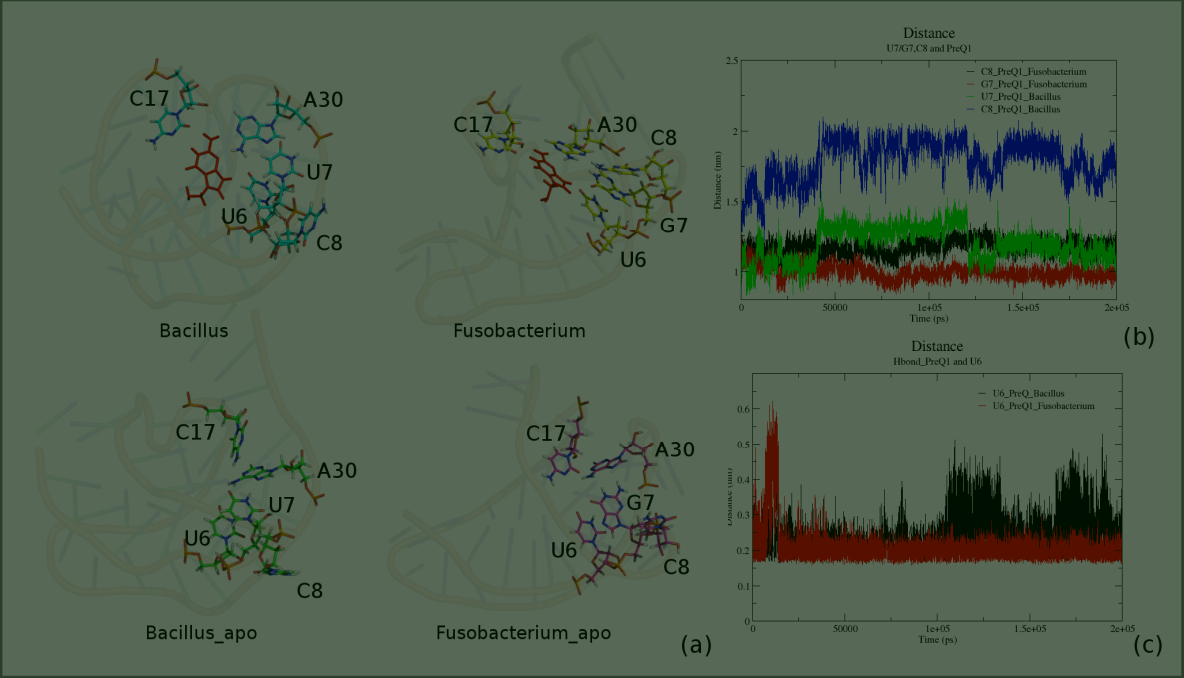

Figure 4. Comparison of the binding pocket of *B. subtilis* and *F. nucleatum* aptamers in bound and apo forms. (a) The final snapshots of bound nucleotides and preQ$_1$ in the different states. (b) The distances between nucleotides from L1 and preQ$_1$ (green and blue lines indicate U7 and C8 of *B. subtilis* aptamer, respectively; red and black lines represent G7 and C8 of *F. nucleatum* aptamer, respectively). (c) The distances of dynamics hydrogen bonds between U6 and preQ$_1$ from *B. subtilis* (black) and *F. nucleatum* (red) over the simulations.

ligand-bound aptamers of *B. subtilis* and *F. nucleatum* with averaged RMSDs around 0.4 nm are relatively stable compared to their ligand-free state with averaged RMSDs around 0.6 nm. The resemblance of the *B. subtilis* and *F. nuclaatum* RMSD data further show that the computer built structure of the *F. nucleatum* preQ$_1$ aptamer is reliable.

Root mean square fluctuation (RMSF) analysis of the 200 ns trajectory compared to starting structures was applied to obtain information on the flexibility of each nucleotide (Fig. 3B). Consistent with a previous simulation study (20) both apo and bound aptamers are very flexible. However, in contrast to the previous simulation study, we found that the L2 regions of apo and bound aptamers are highly flexible, which is consistent with crystallization (10) and NMR studies (9).

Figure 3B also shows that stem P2 is very unstable in the apo form of the *B. subtilis* aptamer but was stabilized in the presence of preQ$_1$ whereas both apo and bound forms were stable, during the 200ns simulation, in the case of *F. nucleatum*. This difference could be due to the different P2 stability of each aptamer. Interestingly, a relatively small but significant difference in fluctuation in the L1 region of both aptamers was observed. Since L1 is involved in preQ$_1$ binding, we decided to focus on interactions

between nts in the binding pocket and $preQ_1$.

Contacts between $preQ_1$ and nucleotides from the binding pocket

To identify which nucleotides interact with the ligand, we analyzed the final structures obtained after 200 ns of MD simulations of apo-preQ1 and preQ1 aptamers of *B. subtilis* and *F. nucleatum*. From comparisons of the binding pocket nucleotides between bound and unbound state (Figure 4A), we conclude that the pairing pattern in the binding pocket is similar to the one determined by NMR spectroscopy of the *B. subtilis* aptamer (9): preQ1 interacts with C17 via its Watson-Crick edge and with U6 and A30 via its sugar side. However, the nucleotides of the binding pocket of *F. nucleatum* aptamer are significantly different (Fig. 4A).

Under NMR conditions the *B. subtilis* U7 and C8 were observed to undergo fast conformational exchange (9). In simulation, we found C8 is far away from $preQ_1$ (Fig. 4A and 4B, blue line) while the distance between U7 and $preQ_1$ was observed that fluctuate between two values (Fig. 4B, green line), in good agreement with NMR study. However, in *F. nucleatum* aptamer, the distances between G7, C8 and preQ1 stay relatively constant and fluctuate less during the course of the MD simulation (Fig. 4B, G7 in red and C8 in black). As shown in Figure 4A, preQ1-U6:G7 tend to form a triplet interaction in the aptamer of *F. nucleatum* that was not observed in the case of *B. subtilis*. This novel interaction may contribute to the higher ligand binding affinity (Fig. 1C) and relatively high stability of G7 (Fig. 4B, red) of the *F. nucleatum* aptamer.

This idea is supported by inspection of the distance of the H-bond between U6, another nucleotide of L1, and $preQ_1$. The hydrogen bond in *F. nucleatum* aptamer was stabilized after 30 ns of MD simulation with averaged distance between 2-3Å (Fig. 4C). However, in the case of *B. subtilis*, the preQ1-U6 distance undergoes fluctuations from 2-5Å in the course of 200 ns of MD simulations (Fig. 4C, black lines). This result further indicates that the preQ1-U6:G7 triple in the *F. nucleatum* aptamer stabilizes the binding pocket and brings U6 close to $preQ_1$.

***In vitro* evidence for the role of the 7^{th} nucleotide in pseudoknot stability**

To support the observation from the MD simulation that the 7^{th} nucleotide may be involved in ligand binding and thereby may affect the stability of pseudoknot structure of the aptamer, we constructed two mutants in which the identity of the 7^{th} nucleotide in both $preQ_1$ aptamers was swapped (Fig. 5) and analyzed these in the frameshift assay. As shown in Figure 5, when G7 of the *F. nucleatum* aptamer was changed to U as in *B. subtilis*, its frameshift efficiency (Fn2) decreased about 5-fold compared to Fn1 (Fig. 1). However, when U7 of the preQ1 aptamer of *B. subtilis* was

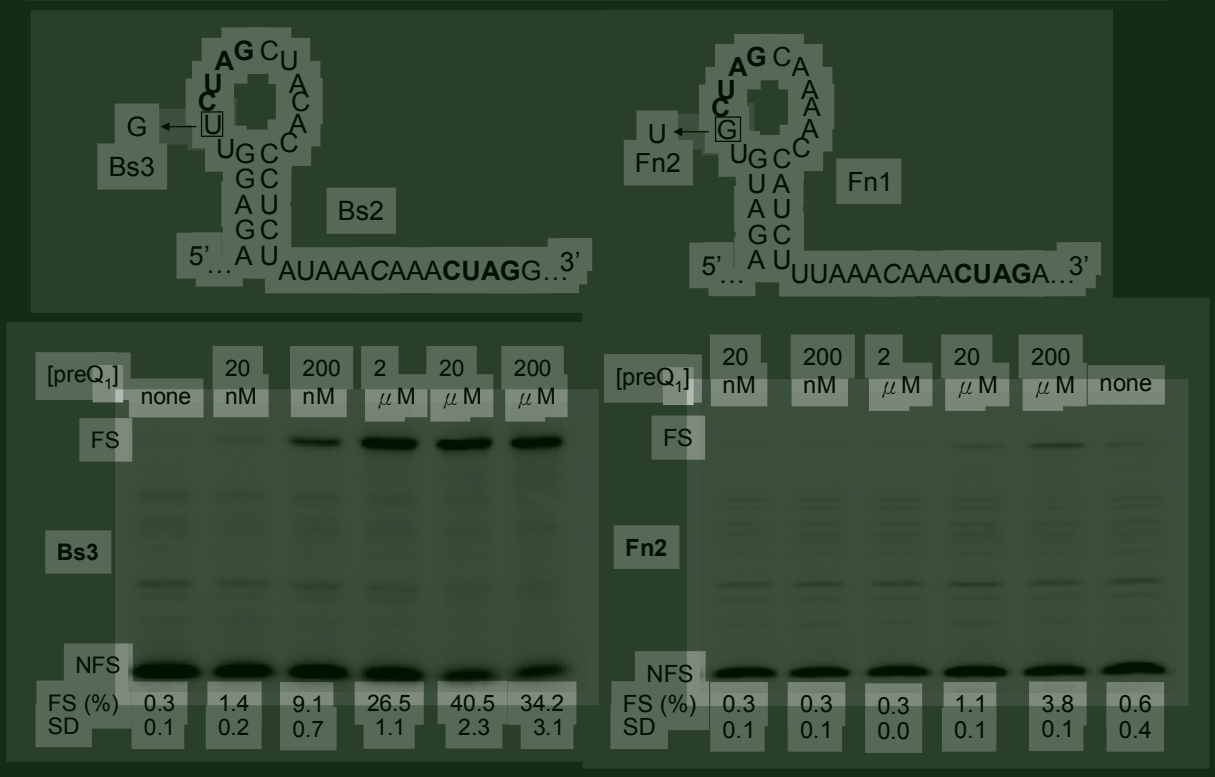

Figure 5. The 7th nucleotide in preQ$_1$ aptamers plays a role in stabilizing ligand-bound pseudoknot structures. The sequence of two mutants at 7th nucleotide position is shown. The bottom pictures show representative ^{35}S-methionine labeled SDS-PAGE. The concentration of added preQ$_1$ and frameshifting efficiency are indicated. See legend to Figure 2 for more details.

mutated to G (Bs3), both the sensitivity and frameshift efficiency were raised about 5-fold with respect to Bs2 (Figure 1). Therefore, our experimental analysis validated the observation from the MD simulation that the 7th nucleotide in preQ1 aptamers of two different species does indeed affect the stability of their ligand-bound pseudoknot structures.

Discussion

We have shown here that preQ$_1$ riboswitch aptamers from *B. subtilis* and *F. nucleatum* can induce significant -1 PRF upon ligand binding. This is quite striking given: i) the presence of an extra 6-nt loop between stems P1 and P2, and ii) the low number of G-C base pairs and low number of total base pairs that are present in the ligand-stabilized pseudoknot. It has been suggested that the first few bps should be G-C to prevent "breathing" of the first stem and efficiently stall ribosomes (15). Moreover, in known natural frameshifter pseudoknots, only the *Sugarcane yellow leaf virus* (ScYLV) frameshift signal has a similarly low GC content (2 AU bps out of 5

bps) in the first stem (21). Resemblance of the preQ1-aptamer to these small luteovirus frameshifter pseudoknots has been noticed by Micura and co-workers (11). In *ScYLV* and *Beet western yellows virus* (BWYV) (22) pseudoknots, the structure is stabilized by interactions between nucleotides in L1 with stem P2 and L3 and P1 (preQ1 aptamer nomenclature). In the solution (9) and crystal (10) structures of preQ1 aptamers in the ligand-bound state, minor groove triples involving adenines of L3 and base pairs of P1 have been observed. These so-called "A-minor" motifs (23) are critical in stabilizing P1(11) and therefore may help P1 to resist unwinding by ribosomal helicase (24) and thus promote frameshifting as discovered in typical frameshifting pseudoknots (25,26). Major groove triples, on the other hand, are even more crucial for luteovirus (27) and telomerase pseudoknots (28). In $preQ_1$ aptamers, interaction of nucleotides from L1 with the C17:$preQ_1$ base pair may be analogous to the luteovirus C-G:C triple (27).

Despite all analogies to luteovirus pseudoknots the presence of a 6-nt loop between stems P1 and P2 in preQ1 aptamers is rarely seen in a frameshifter pseudoknot (see below) as such a loop would have a large destabilizing effect. Apparently in the ligand-bound form, re-organisation of L2 compensates for the destabilizing effect.

The only known frameshifter pseudoknot with a large L2 is found in the ovine Visna-Maedi lentivirus (29) Here 7nts (5'CGUCCGC3') are located between two stems of 7 bps each. Changes in length and composition of L2 appeared detrimental for frameshifting. Possibly, L2, which is invariable in all related small ruminant lentiviruses (Yu & Olsthoorn, unpublished data), is binding some metabolite as well.

It is interesting that these functionally distinct RNA elements have evolved similar motifs to regulate gene expression in a protein-independent manner (4,30). Besides, it has been suggested that the relatively small size of the $preQ_1$ aptamer is generally less likely to be detected using automated searching methods and may comprise a substantial fraction of yet to be discovered riboswitches (6). Taken together, it may suggest that there is an undiscovered frameshift mechanism exploiting riboswitch-like ligand-induced conformational changes to regulate gene expression.

Recently, another riboswitch aptamer was reported to induce -1 PRF in response to its ligand S-adenosylhomocysteine (SAH) (31). However, this study was hampered by the low frameshift efficiency and the lack of an atomic model to correlate mutations in the aptamer to frameshift data.

In our frameshift reporter constructs, the $preQ_1$ aptamers are flanked by long strands of RNA but are nonetheless fully responsive to ligand addition. This may explain that we need higher concentration of preQ1 [reported Kd ~20nM (6)] to induce frameshifting since alternative structures may form under this situation.

However, these constructs may better resemble the natural situation as compared to small synthetic RNAs used in structural studies and binding assays. Moreover, using frameshifting assays to detect ligand-aptamer interactions, although not quantitative, shows not only ligand-dependent but reasonable sensitivity (between 20 nM to 200 nM) and broad dynamic range (20 nM to 200 μM). Since the preQ1 riboswitch is responsible in regulating genes expression of Q synthesis, which is essential for survival, it is probable that we can utilize frameshift assays to select compounds that can bind to preQ1 aptamer to inhibit the growth of pathogens. Furthermore, using a eukaryotic cell-free translation system to monitor prokaryotic RNA-ligand interaction is an advantage to anti-bacterial drug discovery since we can simultaneously monitor potential adverse effects on eukaryotic translation. Thus, using frameshift assays in analyzing preQ1 aptamers may have great potential in high throughout selection of compounds with anti-bacterial activity.

Through computer-assisted simulation, we can build the unresolved *F. nucleatum* $preQ_1$ aptamer structure by the known coordinate of *B. subtilis* $preQ_1$ aptamer with high accuracy (Fig. 3). In agreement with chemical probing and NMR spectroscopy (11), the simulated aptamer does represent a pseudoknot structure in ligand-bound state. A further comparison between the two aptamers shows that the identity of 7th nucleotide affects ligand binding, and this was subsequently confirmed by the frameshift assay. This novel interaction could not have been found without applying this type of research since the atomic-level structure of F. nucleatum aptamer is not available yet. Therefore, this analysis pipeline shows the promising ability to study the structural details of cognate riboswitch aptamers and provides a relatively fast and economical way for designing aptamers with superior ligand binding affinity.

Acknowledgements

We thank Prof. Dr. Dirk Iwata-Reuyl (Portland State University, Portland, United States) for providing us with preQ1 and Uppsala University for running simulation times in Uppmax.

References

1. Wakeman,C.A., Winkler,W.C. and Dann,C.E.,3rd (2007) Structural features of metabolite-sensing riboswitches. *Trends Biochem. Sci.*, **32**, 415-424.

2. Weinberg,Z., Wang,J.X., Bogue,J., Yang,J., Corbino,K., Moy,R.H. and Breaker,R.R. (2010) Comparative genomics reveals 104 candidate structured RNAs from bacteria, archaea, and their metagenomes. *Genome Biol.*, **11**, R31.

3. Thore,S., Leibundgut,M. and Ban,N. (2006) Structure of the eukaryotic thiamine pyrophosphate riboswitch with its regulatory ligand. *Science*, **312**, 1208-1211.

4. Serganov,A. and Patel,D.J. (2007) Ribozymes, riboswitches and beyond: regulation of gene expression without proteins. *Nat. Rev. Genet.*, **8**, 776-790.

5. Bastet,L., Dubé,A., Massé,E. and Lafontaine,D.A. (2011) New insights into riboswitch regulation mechanisms. *Mol. Microbiol.*, **80**, 1148-1154.

6. Roth,A., Winkler,W.C., Regulski,E.E., Lee,B.W.K., Lim,J., Jona,I., Barrick,J.E., Ritwik,A., Kim,J.N., Welz,R., et al. (2007) A riboswitch selective for the queuosine precursor preQ1 contains an unusually small aptamer domain. *Nat. Struct. Mol. Biol.*, **14**, 308-317.

7. Meier,F., Suter,B., Grosjean,H., Keith,G. and Kubli,E. (1985) Queuosine modification of the wobble base in tRNAHis influences “in vivo” decoding properties. *EMBO J.*, **4**, 823-827.

8. Meyer,M.M., Roth,A., Chervin,S.M., Garcia,G.A. and Breaker,R.R. (2008) Confirmation of a second natural preQ1 aptamer class in Streptococcaceae bacteria. *RNA*, **14**, 685-695.

9. Kang,M., Peterson,R. and Feigon,J. (2009) Structural Insights into riboswitch control of the biosynthesis of queuosine, a modified nucleotide found in the anticodon of tRNA. *Mol. Cell*, **33**, 784-790.

10. Klein,D.J., Edwards,T.E. and Ferré-D’Amaré,A.R. (2009) Cocrystal structure of a class I preQ1 riboswitch reveals a pseudoknot recognizing an essential hypermodified nucleobase. *Nat. Struct. Mol. Biol.*, **16**, 343-344.

11. Rieder,U., Lang,K., Kreutz,C., Polacek, N., and Micura, R. (2009) Evidece for pseudoknot formation of class I preQ1 riboswitch aptamers. *Chembiochem*, **4**,

1141-1144.

12. Spitale,R.C., Torelli,A.T., Krucinska,J., Bandarian,V. and Wedekind,J.E. (2009) The structural basis for recognition of the PreQ0 metabolite by an unusually small riboswitch aptamer domain. *J. Biol. Chem.*, **284**, 11012-11016.

13. Farabaugh,P.J. (1996) Programmed translational frameshifting. *Microbiol. Rev.*, **60**, 103-134.

14. Chen,G., Chang,K.-Y., Chou,M.-Y., Bustamante,C. and Tinoco,I.,Jr (2009) Triplex structures in an RNA pseudoknot enhance mechanical stability and increase efficiency of -1 ribosomal frameshifting. *Proc. Natl. Acad. Sci. U.S.A.*, **106**, 12706-12711.

15. Giedroc,D.P., Theimer,C.A. and Nixon,P.L. (2000) Structure, stability and function of RNA pseudoknots involved in stimulating ribosomal frameshifting1. *J. Mol. Biol.*, **298**, 167-185.

16. Olsthoorn,R.C.L., Laurs,M., Sohet,F., Hilbers,C.W., Heus,H.A. and Pleij,C.W.A. (2004) Novel application of sRNA: stimulation of ribosomal frameshifting. *RNA*, **10**, 1702-1703.

17. Yu,C.-H., Noteborn,M.H., Pleij,C.W.A. and Olsthoorn,R.C.L. (2011) Stem-loop structures can effectively substitute for an RNA pseudoknot in -1 ribosomal frameshifting. *Nucleic Acids Res.*, **39**, 8952-8959.

18. Flores,S.C., Wan,Y., Russell,R. and Altman,R.B. (2010) Predicting RNA structure by multiple template homology modeling. *Pac. Symp. Biocompu.t*, 216-227.

19. Zhang,Q., Kang,M., Peterson,R.D. and Feigon,J. (2011) Comparison of solution and crystal structures of preQ1 riboswitch reveals calcium-induced changes in conformation and dynamics. *J. Am. Chem. Soc.*, **133**, 5190-5193.

20. Petrone,P.M., Dewhurst,J., Tommasi,R., Whitehead, L., and Pomerantz, A.K. (2011) Atomic-scale characterization of conformational changes in the preQ1 riboswitch aptamer upon ligand binding. *J. Mol. Graph. Model*, **30**, 179-185.

21. Cornish,P.V., Hennig,M., and Giedroc, D.P. (2005) A loop 2 cytidine-stem 1 minor groove interaction as a positive determinant for pseudoknot-stimulated -1 ribosomal frameshifting. *Proc. Natl. Acad. Sci. U. S. A.*, 102, 12694-12699.

22. Pallan,P.S., Marshall,W.S., Harp,J., Jewett,F.C.3rd, Wawrzak,Z., Brown, B.A.2nd, Rich,A., and Egli,M. (2005) Crystal structure of a luteoviral RNA pseudoknot and

model for a minimal ribosomal frameshifting motif. *Biochemistry*, **44**, 11315-11322.

23. Nissen,P., Ippolito,J.A, Ban,N., Moore,P.B., and Steitz, T.A. (2001) RNA tertiary interactions in the large ribosomal subunit: the A-minor motif. *Proc. Natl. Acad. Sci. U. S. A.*, **98**, 4899-4903.

24. Takyar,S., Hickerson,R.P., and Noller, H.F. (2005) mRNA helicase activity of the ribosome. *Cell*, **120**, 49-58.

25. Su,L., Chen,L., Egli,M., Berger,J.M., and Rich,A. (1999) Minor groove RNA triplex in the crystal structure of a ribosomal frameshifting viral pseudoknot. *Nat. Struct. Biol.*, **6**, 285-292.

26. Olsthoorn,R.C., Reumerman,R., Hilbers,C.W., Pleij,C.W., and Heus,H.A. (2010) Functional analysis of the SRV-1 RNA frameshifting pseudoknot. *Nucleic Acids Res.*, **38**, 7665-7672.

27. Giedroc,D.P., and Cornish,P.V. (2009) Frameshifting RNA pseudoknots: structure and mechanism.*Virus Res.*, **139**, 193-208.

28. Theimer,C.A., Blois,C.A., and Feigon,J. (2005) Structure of the human telomerase RNA pseudoknot reveals conserved tertiary interactions essential for function. *Mol. Cell*, **17**, 671-682.

29. Pennell,S., Manktelow,E., Flatt,A., Kelly,G., Smerdon,S.J., and Brierley, I. (2008) The stimulatory RNA of the Visna-Maedi retrovirus ribosomal frameshifting signal is an unusual pseudoknot with an interstem element. *RNA*, **14**, 1366-1377.

30. ten Dam,E., Brierley,I., Inglis,S., and Pleij,C. (1994) Identification and analysis of the pseudoknot-containing gag-pro ribosomal frameshift signal of simian retrovirus-1. *Nucleic Acids Res.*, **22**, 2304-2310.

31 Chou,M.-Y., Lin,S.-C. and Chang,K.-Y. (2010) Stimulation of -1 programmed ribosomal frameshifting by a metabolite-responsive RNA pseudoknot. *RNA*, **16**, 1236-1244.